THE JOURNAL OF BIOLOGICAL CHEMISTRY VOL. 289, NO. 15, pp. 10582–10591, April 11, 2014

Direct Regulation of Osteocytic Connexin 43 Hemichannels through AKT Kinase Activated by Mechanical Stimulation*[S]

Received for publication, January 16, 2014, and in revised form, February 7, 2014 Published, JBC Papers in Press, February 22, 2014, DOI 10.1074/jbc.M114.550608

Nidhi Batra, Manuel A. Riquelme, Sirisha Burra, Rekha Kar, Sumin Gu, and Jean X. Jiang[1]

From the Department of Biochemistry, University of Texas Health Science Center, San Antonio, Texas 78229-3900

Background: Opening of Cx43 hemichannels by mechanical stress releases factors important for bone remodeling; however, the regulatory mechanism is unknown.
Result: Upon mechanical stimulation, AKT phosphorylates integrin α5 and Cx43, increases interaction, and opens hemichannels.
Conclusion: Phosphorylation of Cx43 and α5 by AKT is critical for hemichannel opening.
Significance: This is the first report demonstrating the functional importance of AKT in regulation of Cx43 hemichannels.

Connexin (Cx) 43 hemichannels in osteocytes are thought to play a critical role in releasing bone modulators in response to mechanical loading, a process important for bone formation and remodeling. However, the underlying mechanism that regulates the opening of mechanosensitive hemichannels is largely unknown. We have recently shown that Cx43 and integrin α5 interact directly with each other, and activation of PI3K appears to be required for Cx43 hemichannel opening by mechanical stimulation. Here, we show that mechanical loading through fluid flow shear stress (FFSS) increased the level of active AKT, a downstream effector of PI3K, which is correlated with the opening of hemichannels. Both Cx43 and integrin α5 are directly phosphorylated by AKT. Inhibition of AKT activation significantly reduced FFSS-induced opening of hemichannels and disrupted the interaction between Cx43 and integrin α5. Moreover, AKT phosphorylation on Cx43 and integrin α5 enhanced their interaction. In contrast to the C terminus of wild-type Cx43, overexpression of the C-terminal mutant containing S373A, a consensus site previously shown to be phosphorylated by AKT, failed to bind with α5 and hence could not inhibit hemichannel opening. Together, our results suggest that AKT activated by FFSS directly phosphorylates Cx43 and integrin α5, and Ser-373 of Cx43 plays a predominant role in mediating the interaction between these two proteins and Cx43 hemichannel opening, a crucial step to mediate the anabolic function of mechanical loading in the bone.

Bone is a living tissue continuously subjected to processes of remodeling which maintains the balance between the amount and spatial organization of the tissue. Mechanical loading or stimulation induced by physical activity is capable of substantially promoting bone remodeling associated with enhancement of morphology and structural properties (1). In general, most bone cells may be involved in mechanosensing. However, theoretical modeling and experimental evidence suggest that osteocytes are the most likely mechanosensors in the bone and shear stress induced by fluid flow shear stress (FFSS)[2] in lacunar-canalicular network is the major mechanism of mechanical loading (2–4). FFSS is likely to stimulate chemical responses, and the signaling molecules generated are likely to be transmitted between the cells by gap junctions and between the cell and the extracellular matrix through the hemichannels (HCs) (5). The activity of HCs has been demonstrated in osteoblasts and osteocytes which respond to mechanical stress (6, 7). In osteocytic MLO-Y4 cells, HCs serve as a portal for the exit of the intracellular anabolic factor, prostaglandin E_2 in response to FFSS (8).

HCs, like gap junctions, are formed from a hexameric array of six connexin molecules and give rise to a half-gap junction channel called HC (9). HCs composed of Cx43 are preferentially closed in cells under resting conditions with very low open probability but apparently sufficient to release physiologically relevant quantities of signaling molecules (*i.e.* ATP, glutamate, NAD^+, prostaglandin E_2) to the external environment (8, 10–12). However, application of positive voltages and changes in protein phosphorylation and/or redox states can increase the open probability of HCs (13). Application of several kinds of external stresses including mechanical, ionic, and ischemic stress results in the activation of connexin HCs. Besides connexin HCs, another type of channel formed by pannexin 1 (Panx1) is known to be activated in response to mechanical stress (14). Panx1 belongs to a family of three membrane proteins (Panx1, Panx2, and Panx3) (15). Compared with Panx2 whose expression is restricted to the brain, and Panx3, predominantly expressed in the skin, connective tissues, and osteoblasts, Panx1 is ubiquitously distributed in most cells and tissues (16). Panx1 channels are large and can be expected to allow the passage of most molecules to which connexin channels are permeable (17). Panx1 channels release ATP to the extracellu-

* This work was supported, in whole or in part, by National Institutes of Health Grants EY012085 and AR46798. This work was also supported by Welch Foundation Grant AQ-1507 (to J. X. J).
[S] This article contains supplemental Figs. S1 and S2.
[1] To whom correspondence should be addressed: Dept. of Biochemistry, University of Texas Health Science Center; 7703 Floyd Curl Dr., San Antonio, TX 78229-3900. Tel.: 210-562-4094; Fax: 210-562-4129; E-mail: jiangj@uthscsa.edu.

[2] The abbreviations used are: FFSS, fluid flow shear stress; AKTi, AKT inhibitor; CT, C-terminal domain; Cx43, connexin 43; HC, hemichannel; IP, immunoprecipitation; LY, Lucifer yellow; Panx, pannexin; RD, rhodamine dextran.

lar medium in response to mechanical stress in *Xenopus* oocytes (14). Each connexin subunit contains four transmembrane domains, two extracellular loops, a cytoplasmic loop, and a C-terminal domain (18). The C-terminal domain varies widely in length and sequence and is thought to play key regulatory roles as well as provide for sites of protein-protein interactions and posttranslational phosphorylation (19). Cx43, the most ubiquitously expressed connexin, is differentially phosphorylated at multiple serine residues throughout its life cycle (20, 21). Phosphorylation of Cx43 is dynamic and changes in response to activation by different kinases, including PKA, PKC, p34cdc2, CKI, MAPK (22). PKB, a Ser/Thr kinase, often known as AKT, has also been shown to phosphorylate Cx43 on Ser-369 and Ser-373 residues (23), but the functional importance is yet unknown. In mammals, three isoforms of AKT (AKT-1, AKT-2, and AKT-3) are present which are independently encoded by three genes (24). We showed recently that mechanical stimulation facilitates the opening of Cx43 HC likely through PI3K activation (25). In this study, we show that integrin α5 and Cx43 are direct substrates of AKT, a major kinase activated by PI3K. AKT phosphorylation of integrin α5 and Cx43 enhances their interaction and maintains the HC in the open state. The AKT phosphorylation residue, Ser-373 of Cx43, plays a major role in the interaction with integrin α5 and HC opening. The regulated opening of HCs could be imperative to anabolic responses of mechanical stimuli on bone tissues by a controlled release of bone modulators. Therefore, AKT conveys mechanical signals to HCs and directly regulates HC function in osteocytes.

EXPERIMENTAL PROCEDURES

Materials—MLO-Y4 osteocytic cells derived from murine long bones were cultured on rat tail collagen type I (0.15 mg/ml) (BD Biosciences)-coated polyester surfaces (Regal Plastics, San Antonio, TX) and were grown in α-modified essential medium (α-MEM) (Invitrogen) supplemented with 2.5% FBS and 2.5% bovine calf serum (Hyclone) and incubated in a 5% CO_2 incubator at 37 °C as described previously (26). SMEM (Invitrogen) was used for dye uptake assay. For immunostaining and dye uptake assays, cells were cultured on glass slides coated with collagen. Antibodies against integrin α5 (R&D Systems, CD49e), phosphoserine/threonine AKT substrate (P/S AKT substrate), pAKT Ser-473, and pAKT Thr-308 (Cell Signaling, MA), Cx43 mouse monoclonal (Santa Cruz Biotechnology) were used. In solution™ AKT inhibitor (AKTi-1/2) VIII selective for isozyme AKT-1/2 used to inhibit activation of AKT was obtained from EMD Biosciences (San Diego, CA). Purified AKT-1 kinase used for *in vitro* phosphorylation was obtained from Cell Signaling. Anti-integrin β1 antibody was a gift from Dr. Alan F. Horowitz (University of Virginia, Charlottesville). Lucifer yellow (LY) and rhodamine dextran (RD) used for dye uptake and dye transfer assay and Alexa Fluor 594- and Alexa Fluor 647-conjugated secondary antibodies were obtained from Invitrogen. Dynabeads® MyOne™ Streptavidin C1 and DPBS with Ca^{2+} and Mg^{2+} were obtained from Invitrogen. Vectashield mounting medium H-1000 was from Vector Laboratories.

Immunoprecipitation and Immunoblotting—Cultured MLO-Y4 cells were collected from 150-mm tissue culture plates and rinsed in lysis buffer (5 mM Tris, 5 mM EDTA/EGTA, pH 8.0) or radioimmunoprecipitation assay buffer and then ruptured by triturating through a 26t[ifrax1,2]-gauge needle 20 times. Lysates were centrifuged at 100,000 × *g* for 30 min at 4 °C. The pellet was resuspended in lysis buffer or radioimmunoprecipitation assay buffer for immunoprecipitation (IP) and co-IP respectively. SDS and Triton X-100 were added to a final concentration of 0.5% each and put on ice for 30 min followed by a brief boiling for 3 min only for IP. Boiled samples were centrifuged for 10 min at 10,000 × *g* to remove the debris. IP buffer was added to the cell lysates to obtain a final concentration of SDS and Triton X-100 to 0.07%. Lysates were precleared with protein G beads (protein G-Sepharose fast flow 4B; Amersham Biosciences) and pelleted by centrifugation at 1800 × *g* at 4 °C for 2 min. Supernatants (precleared lysates) were then incubated with anti-Cx43 or anti-integrin α5 antibody overnight at 4 °C, followed by precipitation of the complexes after incubation at 4 °C with 20 μl of protein G or mouse IgG-agarose beads. Immunoprecipitates were separated on 10% SDS-polyacrylamide gels and immunoblotted with affinity purified anti-Cx43 (E2) (1:300 dilution), anti-phosphoserine AKT substrate antibody (1:1000), anti-integrin α5 (1:1000), or anti-β1 (1:1000) antibody. Blots were developed by enhanced chemiluminescence (Amersham Biosciences).

In Vitro Phosphorylation and Protein Pulldown—Fusion protein was prepared from the GST-tagged C-terminal domain of Cx43 (GST-Cx43-CT) and was *in vitro* phosphorylated with purified AKT-1 kinase using ATP or [γ-^{32}P]ATP. GST alone or *in vitro* reaction without AKT-1 kinase served as a negative control. Reactions were carried out at 30 °C for 30 min and 2 and 4 h and stopped by addition of SDS sample buffer followed by boiling for 5 min. The proteins were resolved on 12% SDS-polyacrylamide gels followed by transfer on nitrocellulose membrane and Western blotting. For ^{32}P-containing samples, gels were dried and exposed to an x-ray film at −80 °C. Protein pulldown experiments were carried out on nonphosphorylated GST-Cx43CT or phosphorylated GST-Cx43CT after *in vitro* phosphorylation reactions as described above using peptide composed of the C terminus of integrin α5. Two biotinylated peptides (each of 27 amino acids in length; >95% purity) were synthesized to cover integrin α5 C terminus (LGFFKRSLPYGTAMEKAQLKPPATSDA-biotin) and a scrambled peptide (LGKSATPYAQFGMLTKASELDPRFKPAK-biotin). Biotinylated peptides were subsequently conjugated to streptavidin-coupled Dynabeads® for 30 min at room temperature. The peptide-conjugated beads were washed with PBS at pH 7.4 and incubated with 10 μg of GST-Cx43CT overnight at 4 °C. After washing with PBS, the binding proteins were eluted in nonreducing SDS sample buffer containing 0.1% SDS, incubation at room temperature for 10 min, and boiling at 95 °C for 5 min. Elutes were separated on 12% SDS-polyacrylamide gels and immunoblotted with affinity-purified anti-Cx43 (C-terminal) (1:300 dilution) or anti-GST antibody (1:5000).

Fluid Flow Shear Stress (FFSS)—Fluid flow was generated by parallel plate flow chambers separated by a gasket of defined thickness with gravity-driven fluid flow using a peristaltic

pump. The thickness of the gasket determines the channel height. By adjusting the channel height and flow rate, stress levels of 16 dynes/cm^2 were generated. Cells were plated in the flow chamber with the surface area of 5 cm^2. Controls consisted of MLO-Y4 cells in SMEM not subjected to FFSS. Each test was conducted for the respective time as indicated. The circulating medium was SMEM. The entire flow system was encased within a large walk-in CO_2 incubator at 5% CO_2 and 37 °C.

Dye Uptake Assay and Inhibition Experiments—MLO-Y4 cells were grown at the density that the majority of the cells were not physically in contact with one another. SMEM, a Ca^{2+}-free medium, was used for fluid flow at 16 dynes/cm^2 for 10 min. Control cells (not subjected to FFSS) were washed three times with SMEM. After FFSS, cells were incubated for dye uptake experiments with 0.2% LY (molecular mass ~547 Da) and 0.2% RD (~10 kDa) dye mixture for 5 min. RD was used as a negative control. Cells were then fixed using 2% paraformaldehyde for 20 min and washed once with PBS before mounting the slides for microscopy. Similar fields were observed under the fluorescence microscope. Dye uptake was determined as a ratio of fluorescent cells to total cells per image. We calibrated the dye uptake results by normalizing the data with unstimulated controls. The fluorescence intensity for unstimulated controls is not zero as a low level of basal dye uptake has been observed. In this case, multiple images from each group were taken, and approximately 100 cells as observed through phase contrast microscopy were counted per group. Similarly, cells that uptake LY or RD were counted. The ratio of the cells that uptake LY dye, but not control cells uptaking RD, and cells observed under phase contrast was calculated. These ratios were normalized to the controls to provide a clear understanding of the -fold increase in dye uptake. Results were expressed as normalized dye uptake (designated as 1) over the respective unstimulated control group. All of our dye uptake experiments were conducted on low density cultures to minimize cell contact with the neighboring cells. We quantified the areas of the cells without visible cell-cell contact. MLO-Y4 cells transfected with GFP-Cx43CT, GFP-Cx43CTS373A, and GFP-Cx43CTS369A,S373A constructs were assayed for dye uptake using a mixture of Alexa Fluor 350 (1 mM) and RD (2%) after subjecting the cells to FFSS.

Generation and Transfection of GFP Constructs Conjugated to C terminus of Cx43 with Wild-type, AKT Single (S373A) or Double Site Mutant (S369A,S373A) into MLO-Y4 Cell—The C terminus of Cx43 encoding the amino acid sequence from 231 to 384 was amplified by PCR and cloned into pcDNA3.1(a) containing GFP to generate the C-terminal Cx43-GFP construct (GFP-Cx43CT). S369A and S373A mutants (GFP-Cx43CTS373A and GFP-Cx43CTS369A,S373A) were generated using the QuikChange™ Site-directed Mutagenesis kit (Qiagen). MLO-Y4 cells were transfected with these constructs and also with GFP alone in pcDNA3.1 construct using Lipofectamine reagent (Invitrogen), and dye uptake was performed. Positive cells for transfection were identified by GFP expression. For protein analysis, the constructs were transfected into the MLO-Y4 cells using the Neon™ transfection system (Invitrogen), and the expression of the endogenous Cx43 and transfected GFP-Cx43CT was determined by Western blotting with our affinity-purified antibody against the C terminus of Cx43 (1:300) or anti-GFP antibody (1:1000) (Abcam).

Co-immunofluorescence—MLO-Y4 cells expressing GFP-Cx43CT or GFP-Cx43CTS373A were cultured as described above, and then cells were cooled on ice for 30 min followed by incubation with polyclonal sheep anti-integrin α5 antibody against secondary extracellular loop domain (1:200 dilution) for 1 h on ice. Cells were washed four times with DPBS with Ca^{2+} and Mg^{2+} (Invitrogen) and then fixed with 2% paraformaldehyde in DPBS at 4 °C for 15 min. The cells were then blocked with 2% goat serum, 1% BSA, and 1% fish gelatin for 1 h at room temperature and then incubated for 1 h at room temperature with polyclonal rabbit anti-Cx43 E2 antibody (1:200 dilutions). The labeling by primary antibodies was detected by incubation with donkey anti-sheep Alexa Fluor 594-conjugated secondary antibody (Invitrogen) for 1 h for integrin α5 and then incubation with donkey anti-rabbit Alexa 647 (Invitrogen) for 1 h for Cx43. Slides were mounted using Vectashield mounting medium (H-1000, Vector Laboratories) and sealed for microscopy. Confocal fluorescence microscopy imaging was performed using a confocal laser scanning microscope (Fluoview; Olympus Optical, Tokyo, Japan). The sequential laser scanning was conducted at a thickness of 0.5 μm. Images were deconvoluted using Iterative deconvolution software of ImageJ, with a known point spread function (for each image 30 iterations were applied with a low pass filter diameter of 0.4 pixel). Brightness and contrast were adjusted off-line to improve clarity for each image; no data were added or deleted. To obtain the Mander's coefficient number, as an index of overlapping of pixels obtained from one channel over another channel, JACoP plugin of ImageJ was used

Statistical Analysis—All of the data were analyzed using GraphPad Prism 5.04 software. One-way analysis of variance and the Student-Newman-Keul test were used for more than two compared groups, and paired Student's *t* test was used for comparison between two groups. Unless otherwise specified in the figure legends, the data are presented as the mean ± S.E. of at least three determinations. *Asterisks* indicate the degree of significant differences compared with the controls (*, $p < 0.05$, **, $p < 0.01$, ***, $p < 0.001$).

RESULTS

AKT Kinase Is Activated in Response to FFSS—We recently showed that inhibition of PI3K activation blocked the HC opening induced by FFSS (25), suggesting the possible involvement of PI3K signaling. Here we showed a significant increase in the levels of active AKT, indicated by AKT phosphorylation at the Ser-473 site after 30 min of FFSS, persisting after 2 h, and then declining from 4 h until reaching the basal non-FFSS level after 24 h (Fig. 1*A*). There is a nonspecific protein band marked with *. This band tends to become faint with fluid flow. We suspect that this could be a nonspecific, "sticky" matrix protein which gets "washed off" by flow. Because FFSS activates AKT, we sought to identify which of the three AKT isoforms was expressed in osteocytic MLO-Y4 cells. Of the three AKT isoforms, AKT-1 and not the other two isoforms, was predominantly expressed in MLO-Y4 cells (Fig. 1*B*). HeLa, C2C12, and

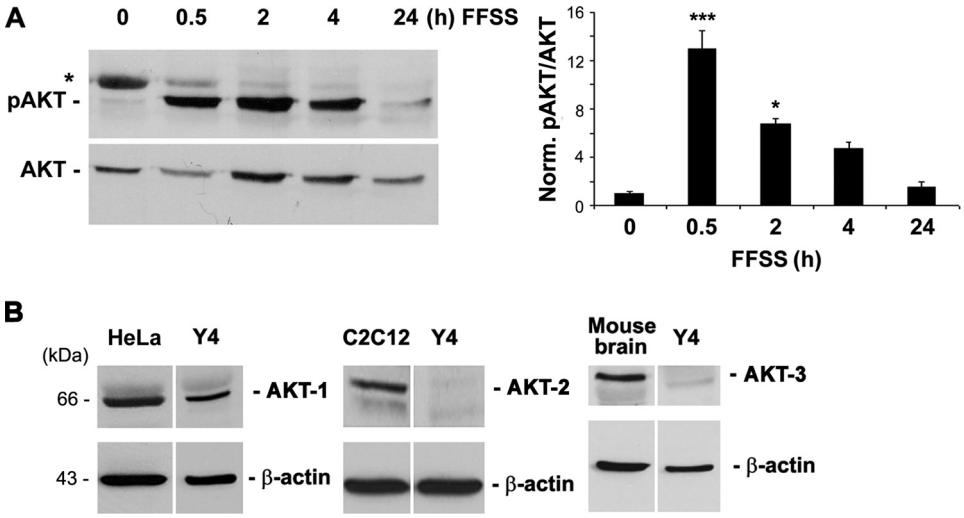

FIGURE 1. **FFSS activated AKT kinase, and AKT-1 is a major isoform expressed in osteocytic MLO-Y4 cells.** *A*, FF increases AKT phosphorylation. MLO-Y4 cells subjected to continuous FFSS for 30 min, 2, 4, and 24 h were analyzed for activation of AKT by immunoblotting the cell lysates with anti-phospho-AKT (Ser-473) antibody. A graph plot using mean band densities of pAKT and total AKT shows that pAKT levels were significantly increased after 30 min of FFSS and gradually declined at 2, 4, and 24 h (*right panel*). 0.5 h *versus* 0 h; ***, $p < 0.001$, $n = 3$. *B*, MLO-Y4 cells primarily express AKT-1 isoform. Lysates of MLO-Y4 cells were immunoblotted with the different anti-AKT isoform antibodies (AKT-1, AKT-2, and AKT-3). Lysates from HeLa cells, C2C12 cells, and mouse brain tissue were used as positive controls for AKT-1, AKT-2, and AKT-3 expression, respectively. *β*-Actin was used as a protein loading control.

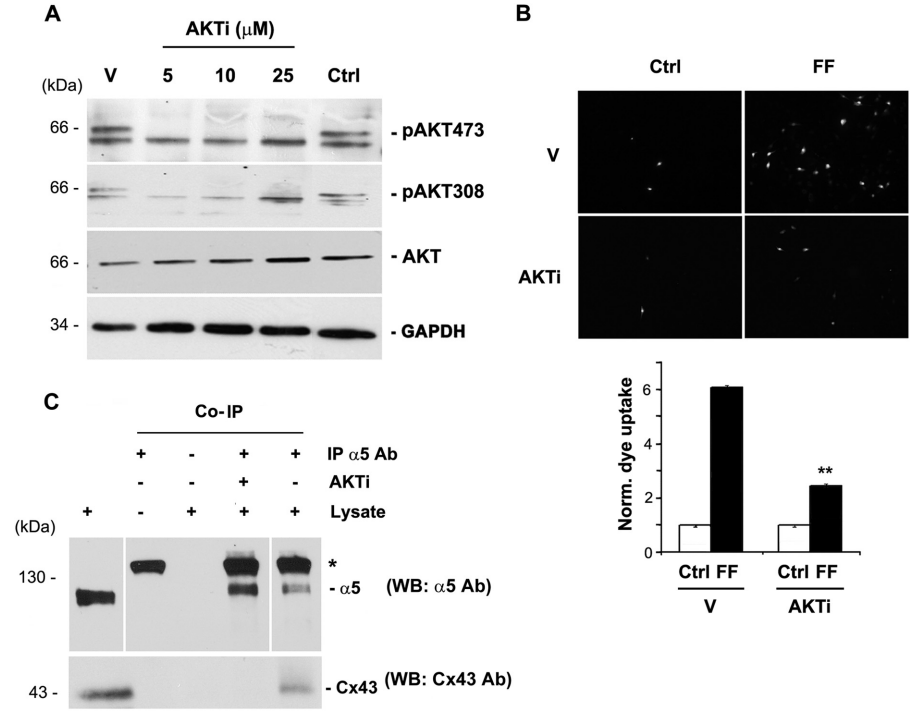

FIGURE 2. **Activated AKT is required for the opening of HCs and the interaction between Cx43 and integrin α5.** *A*, AKT inhibitor blocked the AKT activation. AKT was activated in MLO-Y4 cells by addition of fresh media with serum and treated with an inhibitor which blocked activation of AKT, AKTi at different concentrations ranging from 5 to 25 μM for 1 h. Cell lysates were then immunoblotted with antibodies to the two phosphorylated residues on AKT, Ser-473 and Thr-308, total AKT, and GAPDH. AKTi completely inhibited the phosphorylation on the two sites ($n = 3$). *B*, AKTi blocked FFSS-induced HC opening. LY dye uptake was performed on MLO-Y4 cells under two conditions, treated with AKTi for 1 h (AKTi) and the other not treated with AKTi (Vehicle). Cells treated with either of these conditions were further subjected to FFSS for 30 min (FF) or not (Ctrl). MLO-Y4 cells treated with AKTi and followed by FFSS showed a significant resistance to HC opening in presence of AKTi compared with cells subjected to FFSS directly. FFSS (*AKTi*) *versus* FFSS (vehicle, *V*). **, $p < 0.05$, $n = 3$. *C*, AKTi disrupts the interaction between Cx43 and integrin α5. MLO-Y4 cells were treated with and without AKTi for 1 h, and immunoprecipitation assay was performed using anti-integrin α5 antibody. The immunoprecipitates were immunoblotted with anti-Cx43 or α5 antibody. Cx43 was absent in immunoprecipitates of AKTi-treated cells using anti-α5 antibody ($n = 3$).

mouse brain known to have high expression of AKT-1, 2, and 3, respectively, were used as positive controls.

AKT Activation Is Required for the Interaction between Cx43 and Integrin α5 and Involved in HC Opening by FFSS—To determine whether AKT is involved in the opening of Cx43 HCs, AKTi, an inhibitor specific to the AKT-1 and AKT-2 isoforms, was applied to MLO-Y4 cells after addition of fresh medium with serum. The absence of phosphorylation on the two sites, Ser-473 and Thr-308, confirmed the inactivation of AKT in the presence of the inhibitor (Fig. 2*A*). The effect of

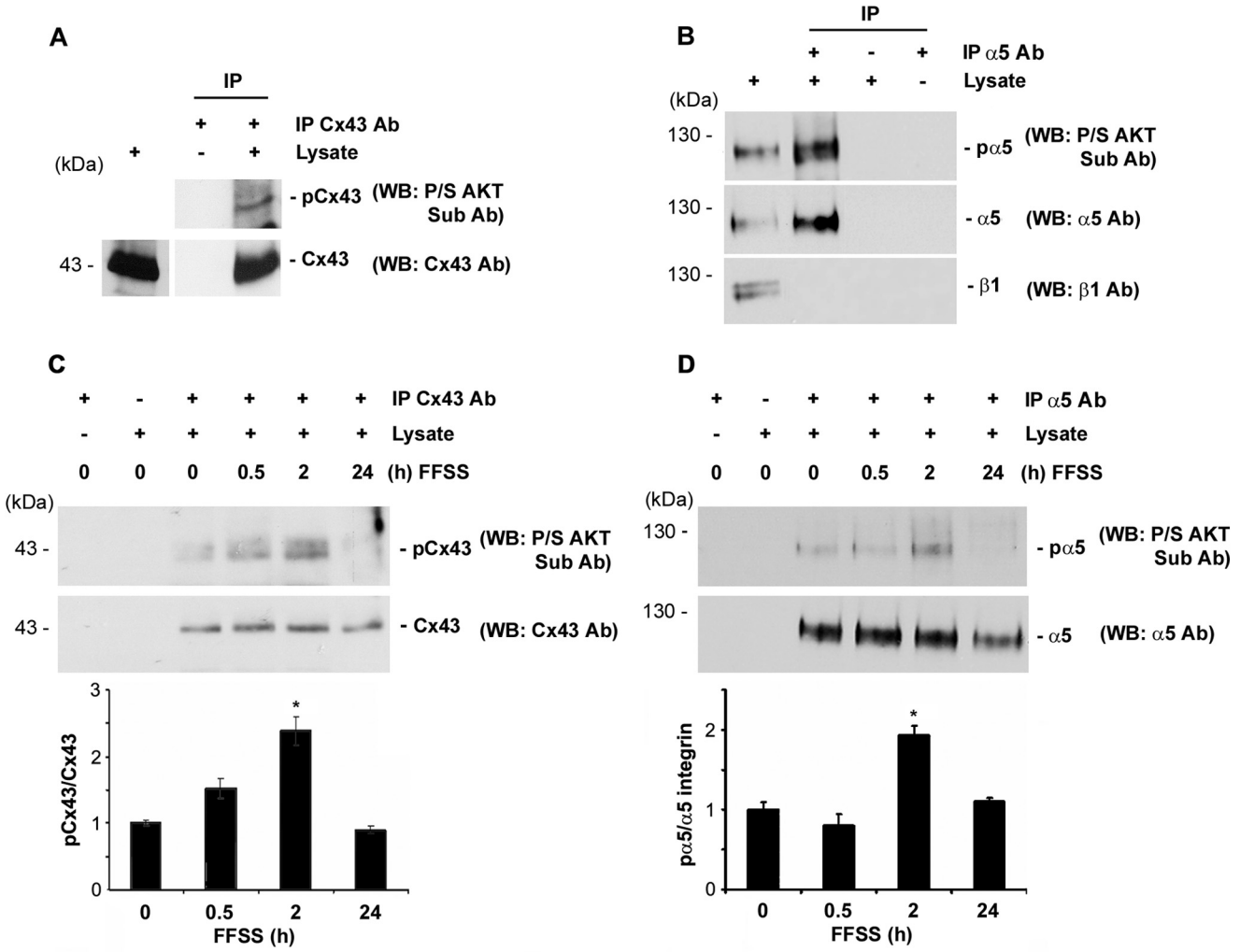

FIGURE 3. **FFSS increases phosphorylation of Cx43 and integrin α5, and both proteins are direct substrates of AKT.** *A*, AKT phosphorylates Cx43 in MLO-Y4 cells. Cx43 was immunoprecipitated from cell lysates using mouse monoclonal anti-Cx43 antibody. Immunoprecipitates were immunoblotted with anti-Pro/Ser AKT substrate or Cx43 antibody. Cx43 in the MLO-Y4 cells was phosphorylated by AKT ($n = 3$). *B*, AKT phosphorylates integrin α5 in MLO-Y4 cells. Integrin α5 from cell lysates was immunoprecipitated using integrin α5 antibody (*IP α5 Ab*), and the immunoprecipitates were immunoblotted (*WB*) using anti-Pro/Ser AKT substrate, integrin α5, or integrin β1 antibody. Immunoprecipitated integrin α5 was a substrate for phosphorylation by AKT ($n = 3$). *C* and *D*, FFSS increases phosphorylation of Cx43 and integrin α5 in MLO-Y4 cells. Cells were subjected to FFSS for different time periods (0, 0.5, 2, and 24 h) and Cx43 and integrin α5 were immunoprecipitated from cell lysates with anti-Cx43 or integrin α5 antibody, respectively, and immunoprecipitates were immunoblotted with Pro/Ser AKT substrate and with Cx43 antibody (*C*) or with integrin α5 antibody (*D*). An increase in phosphorylation of both Cx43 and integrin α5 by AKT was observed after 2 h of FFSS. Graphs were plotted using the ratio of mean band densities of AKT-phosphorylated Cx43 or integrin α5 to total Cx43 or integrin α5, respectively. 2 h *versus* 0 h; *, $p < 0.05$, $n = 3$.

FFSS-activated AKT on HC opening was examined through LY dye uptake assay. Cells were pretreated with AKTi and subjected to FFSS for 30 min, a time point when pAKT levels reach maximal. Inhibition of AKT activation induced by FFSS significantly reduced the opening of Cx43 HCs (Fig. 2*B*). We then asked whether activation of AKT is critical for the interaction between Cx43 and α5. Treatment with AKTi disrupted the interaction between Cx43 and α5 (Fig. 2*C*) as demonstrated through the absence of Cx43 in the immunoprecipitates from AKTi-treated cells using α5 antibody. Our results suggest that activation of AKT induced by FFSS is important for the interaction between Cx43 and integrin α5, and the opening of Cx43 HCs.

Cx43 and Integrin α5 Are Directly Phosphorylated by AKT, and AKT Phosphorylation Enhances the Interaction between These Two Proteins—To determine whether Cx43 and integrin α5 are substrates for AKT kinase, either of the proteins was immunoprecipitated with the respective antibody (Cx43 or α5 antibody), and the elutes were immunoblotted with a motif antibody to AKT-phosphorylated substrates. Both Cx43 and integrin α5 are substrates of AKT as detected by the AKT substrate antibody (Fig. 3, *A* and *B*). To understand how FFSS-activated AKT could possibly influence the phosphorylation of Cx43 and integrin α5, we studied the phosphorylation of Cx43 and integrin α5 mediated by AKT. Lysates collected from different time points of FFSS treatment were immunoprecipitated with either Cx43 or α5 antibody and immunoblotted with anti-Pro/Ser AKT substrate as well as Cx43 or α5 antibody. Phosphorylation on both Cx43 and α5 appeared to increase by nearly 2-fold after 2 h of FFSS (Fig. 3, *C* and *D*) and decreased after 24 h. Cx43 phosphorylation by AKT started to decrease after 4 h (supplemental Fig. S2). These results suggest that Cx43 and integrin α5 are phosphorylated by AKT activated upon FFSS.

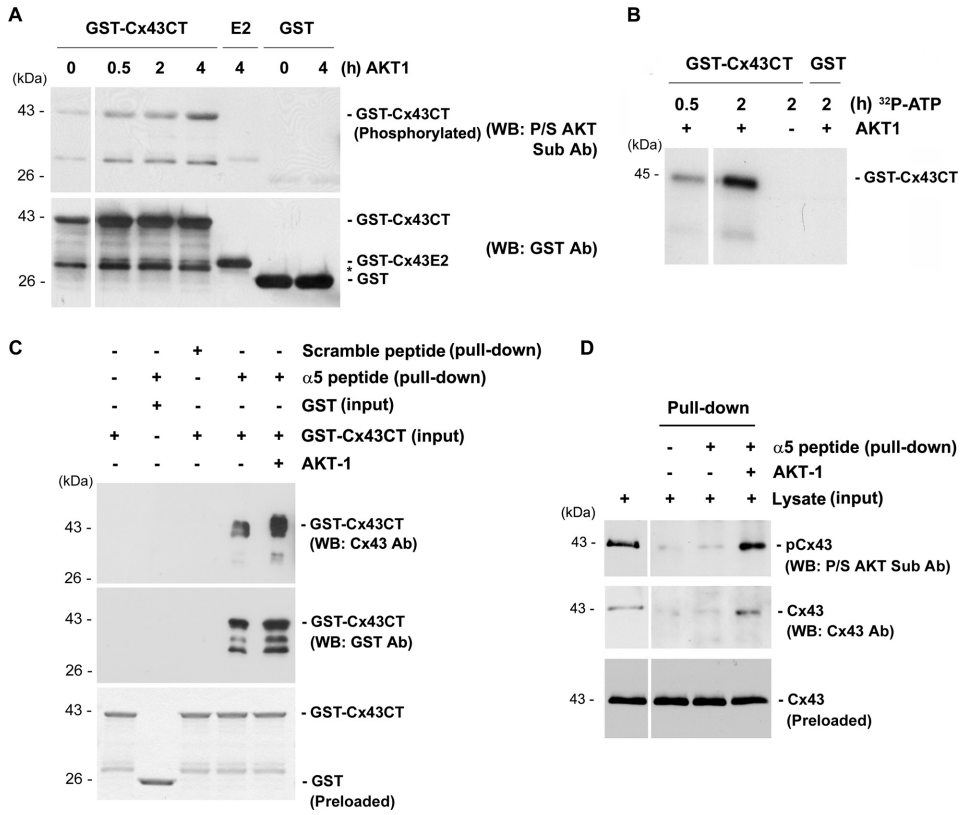

FIGURE 4. **Phosphorylation of the C termini of integrin α5 and Cx43 enhances their interaction.** *A*, *in vitro* phosphorylation of GST-Cx43CT using AKT-1 kinase showed increase in phosphorylation from 30 min to 4 h in GST-Cx43CT, but not in GST-Cx43 (E2) or GST alone ($n = 3$). *B*, *in vitro* phosphorylation of GST-Cx43CT using AKT-1 kinase and [γ-^{32}P]ATP also showed an increase in phosphorylation from 30 min to 2 h. *C*, a dramatic increase in the interaction between GST-Cx43CT and the peptide containing the C terminus of integrin α5 was observed when GST-Cx43CT was phosphorylated by AKT. Protein pulldown was conducted by first treating GST-Cx43CT or GST with AKT-1 kinase for 4 h and then incubating with magnetic beads conjugated with a peptide containing the C terminus of integrin α5 ($n = 3$). *D*, phosphorylation of Cx43 by AKT-1 increased its association with the C terminus of integrin α5. Lysates of MLO-Y4 cell were treated with AKT-1 kinase for 1 h and then incubated with magnetic beads conjugated with a peptide containing C terminus of α5 for pulldown assay.

To determine which domains of Cx43 and α5 are the target sites of phosphorylation by AKT, we performed *in vitro* kinase and pulldown assays. Purified cytoplasmic C-terminal (GST-Cx43CT) and an extracellular loop domain of Cx43 tagged to GST (GST-Cx43E2) were used. The purified AKT-1 kinase phosphorylated GST-Cx43CT in a time-dependent manner. However, this kinase could not phosphorylate either GST-Cx43E2 or GST even after 4 h (Fig. 4*A*). The weak protein bands were observed even without the incubation of AKT, which could be caused by low reactivity of this antibody to nonphosphorylated residue. To further confirm this observation, we conducted an *in vitro* kinase assay using [γ-^{32}P]ATP which would enhance the specificity of the reaction. Consistently, in the presence of AKT-1, only GST-Cx43CT was radioactively labeled by [γ-^{32}P]ATP (Fig. 4*B*). The effect of phosphorylation on the cytoplasmic C-terminal domains of Cx43 and α5 attributing to their interaction was determined by an *in vitro* pulldown assay. In this experiment, the pulldown of GST-Cx43CT was tested with a biotinylated peptide containing the C terminus of integrin α5 attached to the streptavidin beads. The interaction between the two proteins increased greatly upon phosphorylation of the C terminus of Cx43 (Fig. 4*C*). The result was further confirmed through the increased pulldown of Cx43, phosphorylated *in vitro* by AKT-1 kinase from the lysate of MLO-Y4 cells using the peptide containing α5 C terminus (Fig. 4*D*). Together, these results suggest that AKT phosphorylation on the cytoplasmic domains of Cx43 promoted its interaction with integrin α5.

We then addressed whether phosphorylation on either or both Cx43 and α5 was critical for the interaction. We conducted a series of sequential *in vitro* pulldown experiments using purified GST-Cx43CT and α5 C-terminal peptide. When neither of the two proteins was phosphorylated, a low level of interaction was observed (Fig. 5). The level of the interaction increased only when α5 peptide was phosphorylated. However, a dramatic increase in the interaction was observed when GST-Cx43CT was phosphorylated regardless of the phosphorylation state of α5. This result implied that although phosphorylation of α5 enhanced its ability to interact with Cx43, phosphorylation of Cx43 by AKT played a predominant role in the interaction between these two proteins.

Phosphorylation of Ser-373 on Cx43 by AKT Is Critical for the Interaction between Cx43 and Integrin α5 and HC Opening—To identify the site on Cx43 which could be phosphorylated by AKT and be essential for the interaction with α5 thereby affecting the HC opening, we conducted a scansite database search. The analysis revealed two potential AKT phosphorylation sites on the Cx43 C terminus, Ser-369 and Ser-373, the latter having a higher probability (within the top 2% (1.178%)) of potential AKT phosphorylation sites). This analysis is consistent with a

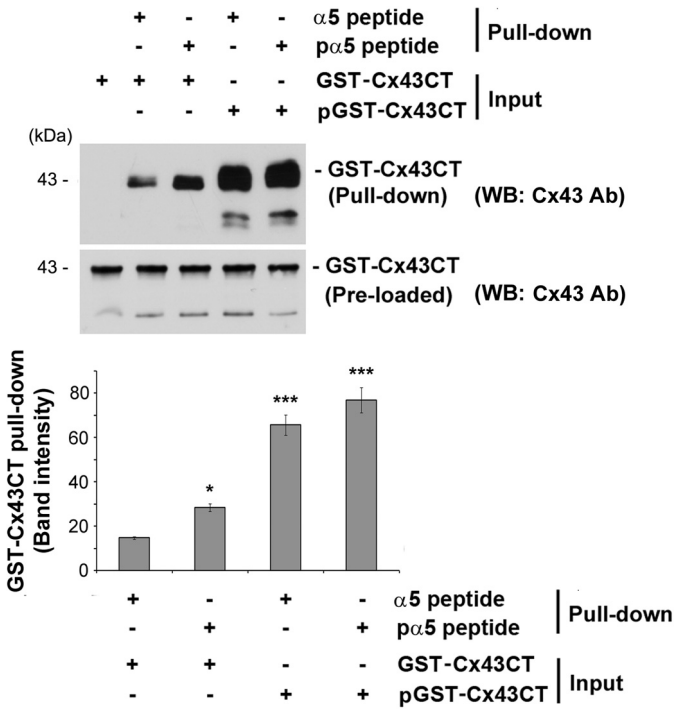

FIGURE 5. **Phosphorylation of the C terminus of Cx43 by AKT plays a predominant role in its interaction with integrin α5.** Purified GST-Cx43CT and/or a peptide containing the C terminus of α5 (α5 peptide) conjugated with magnetic beads was incubated with and without AKT-1 kinase for 4 h. Elutes and inputs from the pulldown assay were immunoblotted (*WB*) with anti-Cx43 antibody. The band intensity was quantified showing a drastic increase in the interaction between GST-Cx43CT and the peptide containing the C terminus of integrin α5 when GST-Cx43CT was phosphorylated by AKT-1. Non-AKT-1-treated (first column) *versus* all other conditions; *, $p < 0.05$; ***, $p < 0.001$, $n = 3$.

previous report of the phosphorylation of Ser-373 by AKT (23). GFP constructs were generated containing the wild-type Cx43 (GFP-Cx43CT), S373A single site mutant (GFP-Cx43CTS373A), or S369A,S373A double site mutant (GFP-Cx43CTS369A,S373A). These exogenous GFP fusion proteins were similarly expressed in MLO-Y4 cells (Fig. 6*A*). The AKT phosphorylation of S373A mutant was investigated by immunoprecipitation of Cx43 from lysate of cells transfected with either GFP-CTCx43 or GST-CTS373A. The S373A mutation significantly reduced the phosphorylation by AKT compared with the wild-type Cx43 (Fig. 6*B*, *right panel*). This result suggested that Ser-373 on Cx43 is a major target for phosphorylation by AKT.

To determine the functional importance of the phosphorylation of Ser-373 by AKT, we overexpressed GFP-conjugated Cx43CT mutant S373A as well as GFP-Cx43CT in MLO-Y4 cells. Unlike GFP-Cx43CT, the S373A mutant did not affect the opening of HCs induced by FFSS (Fig. 7*A*). Furthermore, we also showed that mutations of both AKT consensus sites, S369A and S373A, failed to block HC opening induced by FFSS, similar to the single S373A mutation. We further determined the interaction of α5 with Cx43, GFP-Cx43CT, or mutant in cells exogenously expressing GFP-Cx43CT or GFP-Cx43CTS373A. Comparable levels of expression were shown in cells expressing exogenous wild-type or mutant of GFP-Cx43CT (Fig. 7*B*, *top panel*). Similar as we recently reported (25), an IP assay using α5 antibody showed that GFP-Cx43CT was able to interact with endogenous α5 (Fig. 7*B*, *bottom panels*). The mutation S373A reduced the interaction between Cx43CT and α5. To further confirm the role of Ser-373 residue of Cx43, we performed immunofluorescence by co-labeling MLO-Y4 cells expressing GFP-Cx43CT or GFP-Cx43CTS373A with antibodies against Cx43 and α5

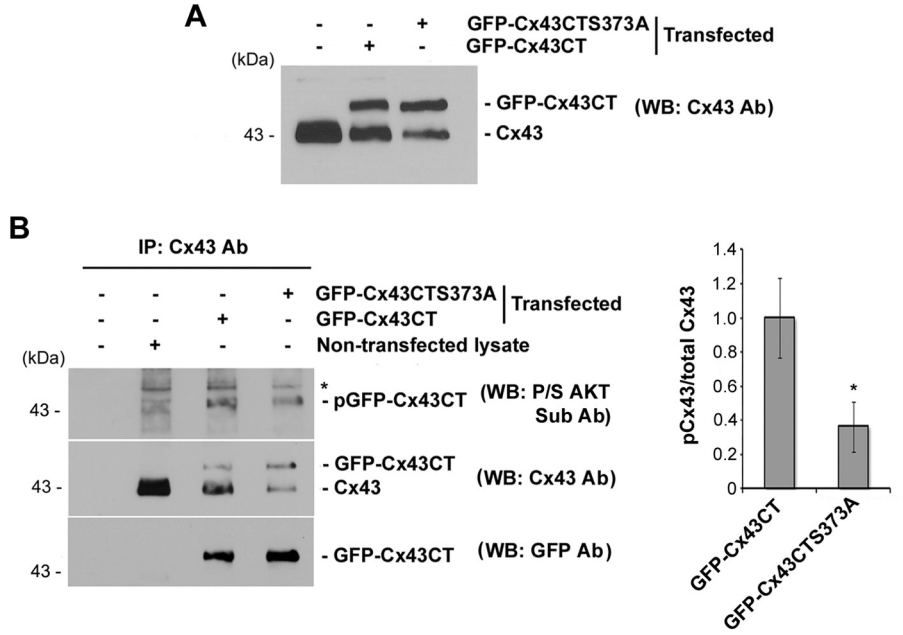

FIGURE 6. **Ser-373 on the C terminus of Cx43 is a major site for phosphorylation of AKT on Cx43.** *A*, exogenous GFP fusion proteins containing Cx43CT and Cx43CTS373A mutants were comparably expressed in MLO-Y4 cells. Cell lysates transfected with Cx43CT or Cx43CTS373A were immunoblotted (*WB*) with anti-Cx43 antibody. *B*, Ser-373 on Cx43 is a major site for AKT phosphorylation. Either GFP-Cx43CT or GFP-Cx43CTS373A was exogenously expressed in MLO-Y4 cells. Cell lysates were immunoprecipitated using anti-Cx43 antibody. Immunoprecipitates were immunoblotted with antibodies to P/S AKT substrate (*top panel*), Cx43 (*middle panel*), or GFP (*bottom panel*). Intensity of the band was quantified (*right panel*). GFP-Cx43CT *versus* GFP-Cx43CTS373A; *, $p < 0.05$, $n = 3$.

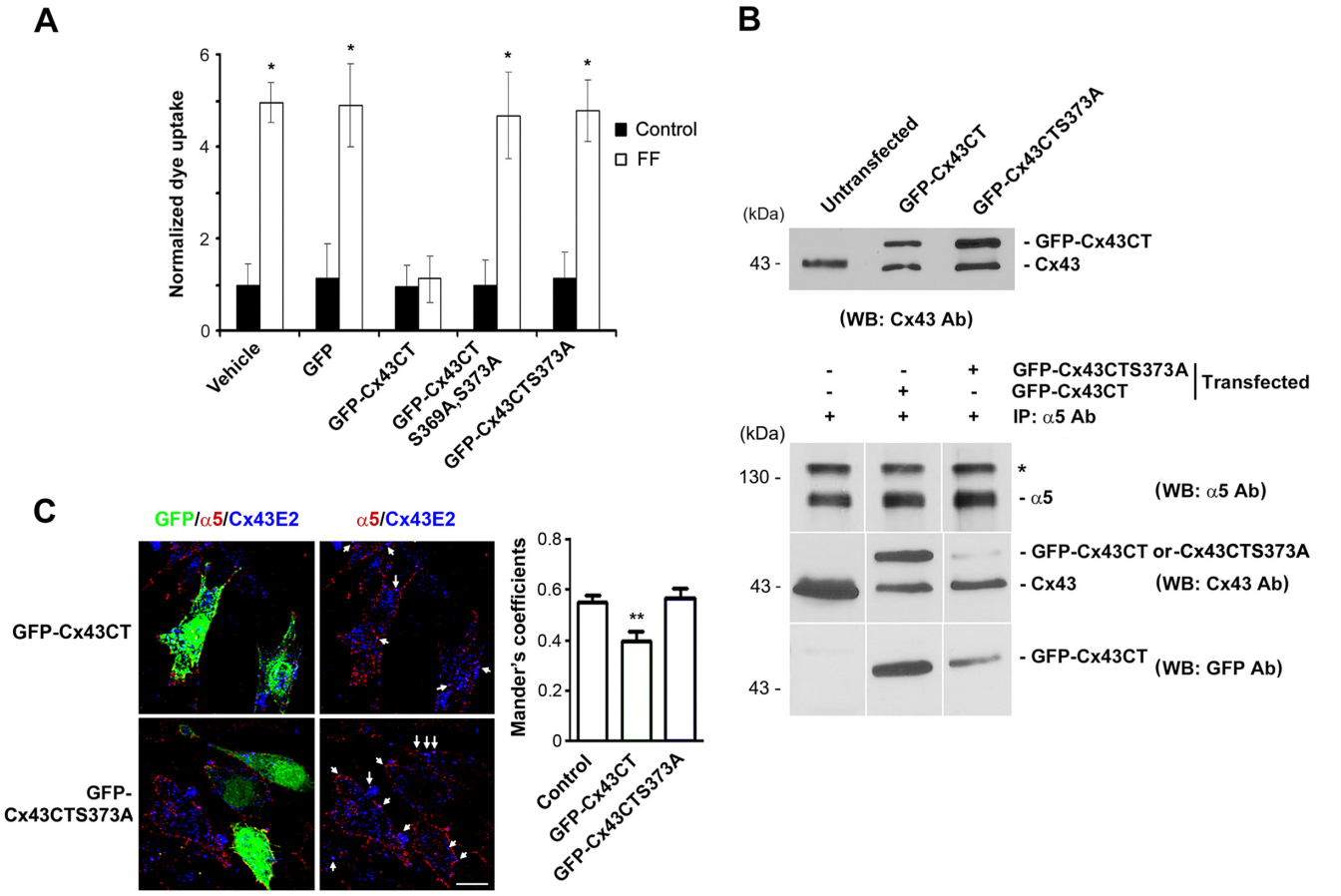

FIGURE 7. **Ser-373 on Cx43 is critical for the interaction of Cx43 with integrin α5 and HC opening.** *A*, S373A mutation on Cx43 failed to inhibit HC opening induced by FFSS. MLO-Y4 cells transfected with DNA constructs containing GFP-Cx43CT, GFP-Cx43CTS373A, GFP-Cx43CTS369A,S373A, GFP, or vector alone were subjected to FFSS for 15 min or non-FFSS static controls. Uptake assay was performed with Alexa Fluor 350 dye and RD. The number of cells with GFP signals that took up the dye were counted and quantified. Cells expressing GFP-Cx43CT, but not GFP-Cx43CTS373A, GFP-Cx43CTS369A,S373A, or vehicle control, showed reduction in dye uptake in response to FFSS. GFP-Cx43CT *versus* all other conditions; *, $p < 0.05$, $n = 3$. *B*, S373A mutation reduced Cx43CT binding to integrin α5. Lysates of MLO-Y4 cells exogenously expressing GFP-Cx43CT or GPF-Cx43CTS373A were immunoblotted using anti-Cx43 antibody. Cell lysates were immunoprecipitated with anti-α5 antibody, and immunoprecipitates were immunoblotted (*WB*) with antibody to α5 (*top panel*), Cx43 (*middle panel*), or GFP (*lower panel*) $n = 3$. *C*, reduction of the co-localization between integrin α5 and Cx43 with the expression of GFP-Cx43CT, but not GFP-Cx43CTS373A. MLO-Y4 cells transfected with DNA constructs containing GFP-Cx43CT or GFP-Cx43CTS373A were co-immunofluorescence labeled with anti-integrin α5 (*red*) and Cx43E2 (against E2 domain) (*blue*) antibodies (*left panels*). The transfected cells are indicated by GFP fluorescence. The co-localized signals are indicated by *white arrows*. The extent of co-localization on the cell surface was analyzed using ImageJ (*right panel*). GFP-Cx43CT *versus* control (untransfected) and GFP-Cx43CTS373A; **, $p < 0.01$, $n = 20$. *Scale bar*, 10 μm.

(Fig. 7*C*, *left panels*). The extent of co-localization of α5 and Cx43 on the cell surface was quantified (Fig. 7*C*, *right panel*). Because only a certain percentage of the cells were transfected, we quantified the extent of co-localization in the transfected and nontransfected cells separately. We found that the degree of overlapping signals indicated by Mander's coefficients was significantly reduced in the cells expressing GFP-Cx43CT, but not in the cells expressing GFP-Cx43CTS373, which is similar to nontransfected control cells. These results suggest that Ser-373 of Cx43 is important for its interaction with integrin α5 and the opening of HCs in response to FFSS. Thus, the residue Ser-373 of Cx43 is a primary site involved in HC opening because of its phosphorylation by AKT and interaction with integrin α5.

DISCUSSION

Post-translational modification has been shown to play an important role in gap junction channel assembly and function. However, there is scarce information regarding the regulation of HC opening. Moreover, Cx43 HC is a mechanosensitive channel, but how this channel is regulated in response to mechanical signals is largely unknown. As discussed above, in addition to Cx43 HC, there are Panx1-forming HCs, which have been shown to open in response to mechanical perturbation when examined in *Xenopus* oocytes (14) We noticed the expression of Panx 1 in osteocytes (supplemental Fig. S1); however, our earlier study showed that Cx43 siRNA or an antibody to the extracellular loop of Cx43 specifically blocks the Cx43 HC opening and prevents the release of prostaglandin E_2 in osteocytic cells (8, 27). These data suggest that Cx43 HC plays a predominant role in osteocytes in response to mechanical loading. Here, we elucidate the molecular mechanism that regulates the opening of Cx43 HC by AKT activated by mechanical stimulation. Most previous studies have shown that phosphorylated Cx43 is responsible for closure of gap junctions or HCs (20, 22). Our study shows that AKT phosphorylation of Cx43 has a positive role on the HCs by maintaining this channel in an open state. We discern the mechanistic link between the direct phos-

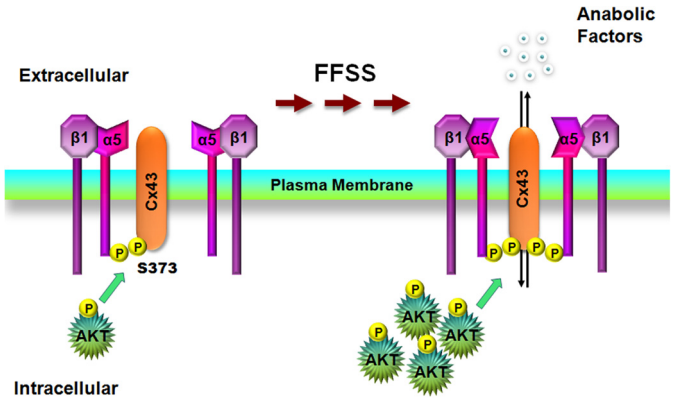

FIGURE 8. **Illustration of the role of AKT activation by FFSS regulates Cx43 interaction with integrin α5 and HC opening.** Under non-FFSS static conditions, there are low levels of basal AKT which mediates phosphorylation on Cx43 and integrin α5 and promotes weak interaction between these two proteins. FFSS activates AKT which leads to the phosphorylation of Cx43 and α5 and enhancement of the interaction between these two proteins and a possible conformational activation of α5 (25). The interaction and activation lead to the opening of HCs in osteocytes which may associate with the release of small autocrine/paracrine factors important for bone formation and remodeling in response to mechanical loading.

phorylation of Cx43 and integrin α5 by AKT, the interaction between these two proteins and the mechanical stimulation induced opening of Cx43 HCs. We report three major findings in this study. (i) FFSS activates AKT, and this activation is critical for Cx43 HC opening. (ii) Both Cx43 and integrin α5 are directly phosphorylated by AKT, and FFSS increased the phosphorylation of both proteins. (iii) Phosphorylation by AKT enhanced the interaction between Cx43 and integrin α5, and the AKT phosphorylation site, Ser-373 on Cx43, is critical for the interaction with integrin α5 and HC opening. Based on our previous and current studies, a model is proposed, as illustrated in Fig. 8 for the functional involvement of AKT and the effect of AKT phosphorylation of Cx43 and integrin α5 on the interaction of these two proteins and HC opening in the mechanically stimulated osteocytic cells. Under nonstimulated conditions, there is a basal level of AKT activation, and low levels of Cx43 and integrin α5 are phosphorylated, which aids the interaction between these two proteins. Upon FFSS, the interaction between these two proteins is greatly enhanced because of a rise in the level of activated AKT, leading to an increase in the phosphorylation of Cx43 and α5. Therefore, as long as elevated active AKT levels are sustained by FFSS, the two proteins would remain associated, which keeps the HCs in the open state. Continuous FFSS from 30 min to 24 h clearly showed that the rise in pAKT levels began at an early time, peaked at 30 min, and was maintained for 2 h which then declined from 4 h to reach to the level similar to a nonstimulated state. Interestingly, the maximal level of Cx43 phosphorylation occurs after 2 h. Given that Cx43 phosphorylation is a continuous process, the cumulative levels of phosphorylated Cx43 ought to be higher after 2 h than 30 min under the condition that the dephosphorylation process is less dominant within the 2-h period. Here, we measured the total phosphorylated Cx43, but not the rate of phosphorylation. Therefore, this time lag could be a combined outcome of accumulated Cx43 phosphorylation by AKT and dephosphorylation by phosphatase. In our previous studies, we measured the activities of Cx43 hemichannels at 30 min and 2 h of FFSS and found that at both time points the dye uptake was significantly increased with slightly more increase at 2 h than 30 min of FFSS (27). Thus, the time frame of Cx43 phosphorylation is consistent with that of HC opening. Our results clearly show that activated AKT is critical for HC opening because AKTi blocked the opening and disrupted the interaction between Cx43 and α5. Whereas phosphorylation of Cx43 by AKT has been reported in EGF-treated cells (23), we showed that in osteocytic MLO-Y4 cells, FFSS not only promotes the phosphorylation of Cx43 by AKT, but also integrin α5. Although phosphorylation of α5 enhances the interaction to certain degree, AKT-phosphorylated Cx43 plays a predominant role in its interaction with α5 and the function of HCs.

There are two consensus sites for AKT on Cx43, Ser-369 and Ser-373. These AKT substrate sequences (*RXRXX*(S/T)) might overlap with the consensus sites of other kinases that phosphorylate Cx43, such as PKA whose target sites may be Ser-265, Ser-368, Ser-369, and Ser-373 on Cx43 (28). However, activation of AKT by FFSS, specific inhibition of active AKT by AKT inhibitor, and direct phosphorylation of Cx43 by AKT-1 suggest that regulation of HC opening is mediated by AKT, but unlikely by other mechanisms. Direct phosphorylation on Cx43 is likely to modulate the gating of HCs. Alternatively, it may affect Cx43 interaction with other protein(s), which in turn influences HC function.

In accordance with the observation in the cell, *in vitro* pull-down studies using purified AKT-1 kinase, a predominant AKT isoform present in MLO-Y4 cells, phosphorylated the cytoplasmic domains of Cx43 and α5 and promoted their interaction, where phosphorylation on Cx43 appeared to play a predominant role. Consistently, FFSS enhanced the phosphorylation of both Cx43 and α5, possibly accounting for the increase in the interaction between these proteins in response to FFSS as reported in our recent study (25). We showed that phosphorylation on Ser-373 of Cx43 is critical for the interaction because ablation of this phosphorylation by the mutation disrupts the interaction with α5. These data implicate that Ser-373 on Cx43 is important for the interaction with α5 and opening of HC. Although, at this stage, we have limited information about the site on α5 which is phosphorylated by AKT, phosphorylation on α5 appears to play lesser important roles in its interaction with Cx43.

As opening of HCs is a well controlled process for the release of bone modulators, it is imperative to understand the mechanism involved in the regulation of HCs that allows an appropriate efflux of molecules, critical to bone formation and remodeling under mechanical stimulation. Further studies will direct the understanding of how phosphorylation of Cx43 on a specific residue strengthens the protein-protein interaction on the molecular and structural basis.

Acknowledgments—We thank Dr. Gregg B. Fields for the generation of biotinylated peptides to the C terminus of integrin α5, Dr. Eugene Sprague and Jian Luo for assistance in fluid flow experiments, Tommy Nguyen for technical assistance, and the members of Dr. Jiang's laboratory for critical reading of the paper and valuable comments.

REFERENCES

1. Srinivasan, S., Gross, T. S., and Bain, S. D. (2012) Bone mechanotransduction may require augmentation in order to strengthen the senescent skeleton. *Ageing Res. Rev.* **11,** 353–360
2. Aarden, E. M., Burger, E. H., and Nijweide, P. J. (1994) Function of osteocytes in bone. *J. Cell. Biochem.* **55,** 287–299
3. Burger, E. H., and Klein-Nulend, J. (1999) Mechanotransduction in bone: role of the lacunocanalicular network. *FASEB J.* **13,** S101–112
4. Cowin, S. C., Moss-Salentijin, L., and Moss, M. L. (1991) Candidates for the mechanosensory system in bone. *J. Biomed. Eng.* **113,** 191–197
5. Jiang, J. X., Siller-Jackson, A. J., and Burra, S. (2007) Roles of gap junctions and hemichannels in bone cell functions and in signal transmission of mechanical stress. *Front. Biosci.* **12,** 1450–1462
6. Romanello, M., Pani, B., Bicego, M., and D'Andrea, P. (2001) Mechanically induced ATP release from human osteoblastic cells. *Biochem. Biophys. Res. Commun.* **289,** 1275–1281
7. Cheng, B., Zhao, S., Luo, J., Sprague, E., Bonewald, L. F., and Jiang, J. X. (2001) Expression of functional gap junctions and regulation by fluid flow shear stress in osteocyte-like MLO-Y4 cells. *J. Bone Miner. Res.* **16,** 249–259
8. Cherian, P. P., Siller-Jackson, A. J., Gu, S., Wang, X., Bonewald, L. F., Sprague, E., and Jiang, J. X. (2005) Mechanical strain opens connexin 43 hemichannels in osteocytes: a novel mechanism for the release of prostaglandin. *Mol. Biol. Cell* **16,** 3100–3106
9. Goodenough, D. A., and Paul, D. L. (2003) Beyond the gap: functions of unpaired connexin channels. *Nat. Rev. Mol. Cell Biol.* **4,** 285–294
10. Stout, C. E., Costantin, J. L., Naus, C. C., and Charles, A. C. (2002) Intercellular calcium signaling in astrocytes via ATP release through connexin hemichannels. *J. Biol. Chem.* **277,** 10482–10488
11. Ye, Z. C., Wyeth, M. S., Baltan-Tekkok, S., and Ransom, B. R. (2003) Functional hemichannels in astrocytes: a novel mechanism of glutamate release. *J. Neurosci.* **23,** 3588–3596
12. Bruzzone, S., Guida, L., Zocchi, E., Franco, L., and De Flora, A. (2001) Connexin 43 hemichannels mediate Ca^{2+}-regulated transmembrane NAD^{+} fluxes in intact cells. *FASEB J.* **15,** 10–12
13. Sáez, J. C., Retamal, M. A., Basilio, D., Bukauskas, F. F., and Bennett, M. V. (2005) Connexin-based gap junction hemichannels: gating mechanisms. *Biochim. Biophys. Acta* **1711,** 215–224
14. Bao, L., Locovei, S., and Dahl, G. (2004) Pannexin membrane channels are mechanosensitive conduits for ATP. *FEBS Lett.* **572,** 65–68
15. Bruzzone, R., Hormuzdi, S. G., Barbe, M. T., Herb, A., and Monyer, H. (2003) Pannexins, a family of gap junction proteins expressed in brain. *Proc. Natl. Acad. Sci. U.S.A.* **100,** 13644–13649
16. Penuela, S., Gehi, R., and Laird, D. W. (2013) The biochemistry and function of pannexin channels. *Biochim. Biophys. Acta* **1828,** 15–22
17. Pelegrin, P., and Surprenant, A. (2006) Pannexin-1 mediates large pore formation and interleukin-1β release by the ATP-gated $P_{2X7\ receptor}$. *EMBO J.* **25,** 5071–5082
18. Willecke, K., Eiberger, J., Degen, J., Eckardt, D., Romualdi, A., Güldenagel, M., Deutsch, U., and Söhl, G. (2002) Structural and functional diversity of connexin genes in the mouse and human genome. *Biol. Chem.* **383,** 725–737
19. Hervé, J. C., Bourmeyster, N., and Sarrouilhe, D. (2004) Diversity in protein-protein interactions of connexins: emerging roles. *Biochim. Biophys. Acta* **1662,** 22–41
20. Lampe, P. D., and Lau, A. F. (2004) The effects of connexin phosphorylation on gap junctional communication. *Int. J. Biochem. Cell Biol.* **36,** 1171–1186
21. Solan, J. L., and Lampe, P. D. (2005) Connexin phosphorylation as a regulatory event linked to gap junction channel assembly. *Biochim. Biophys. Acta* **1711,** 154–163
22. Solan, J. L., and Lampe, P. D. (2009) Connexin 43 phosphorylation: structural changes and biological effects. *Biochem. J.* **419,** 261–272
23. Park, D. J., Wallick, C. J., Martyn, K. D., Lau, A. F. J. C., and Warn-Cremer, B. J. (2007) Akt phosphorylates connexin43 on Ser373, a "model-1" binding site for 14-3-3. *Cell Commun. Adhes.* **14,** 211–226
24. Franke, T. F., Hornik, C. P., Segev, L., Shostak, G. A., and Sugimoto, C. (2003) PI3K/Akt and apoptosis: size matters. *Oncogene* **22,** 8983–8998
25. Batra, N., Burra, S., Siller-Jackson, A. J., Gu, S., Xia, X., Weber, G. F., DeSimone, D., Bonewald, L. F., Lafer, E. M., Sprague, E., Schwartz, M. A., and Jiang, J. X. (2012) Mechanical stress-activated integrin $\alpha5\beta1$ induces opening of connexin 43 hemichannels. *Proc. Natl. Acad. Sci. U.S.A.* **109,** 3359–3364
26. Kato, Y., Windle, J. J., Koop, B. A., Mundy, G. R., and Bonewald, L. F. (1997) Establishment of an osteocyte-like cell line, MLO-Y4. *J. Bone Miner. Res.* **12,** 2014–2023
27. Siller-Jackson, A. J., Burra, S., Gu, S., Xia, X., Bonewald, L. F., Sprague, E., and Jiang, J. X. (2008) Adaptation of connexin 43-hemichannel prostaglandin release to mechanical loading. *J. Biol. Chem.* **283,** 26374–26382
28. Yogo, K., Ogawa, T., Akiyama, M., Ishida-Kitagawa, N., Sasada, H., Sato, E., and Takeya, T. (2006) PKA implicated in the phosphorylation of Cx43 induced by stimulation with FSH in rat granulosa cells. *J. Reprod. Dev.* **52,** 321–328